Magnetoresistive Biosensors for On-Chip Detection and Localisation of Paramagnetic Particles

Zhaochen Yin, *Student Member, IEEE*, Edoardo Bonizzoni, *Member, IEEE*, and Hadi Haidari, *Senior Member, IEEE*

***Abstract* —** This paper presents the design and the implementation of an on-chip magnetoresistive sensors array for cell detection and localisation. Giant magnetoresistance (GMR) sensors have been used due to their high sensitivity and resolution. A new calibration and localisation algorithm has been coded and implemented. In order to generate the required homogenous magnetic field, a custom 3D printed Halbach cylinder has been simulated and characterised. The system includes sensory and electronic boards to collect the data and to transfer them to a computing server. The experimental results are displayed in a visual interface. Ferrofluid is used to model and simulate the magnetic field change of the cell. This paper demonstrates a 4×4 sensors array and provides a step towards the miniaturised on-chip magnetoresistive-based cell detection and localisation for portable diagnostics applications.

***Keywords* — Magnetic Biosensors, Giant Magnetoresistive (GMR), Lab-on-Chip, Detection, Localisation, Paramagnetic Particles, Point of Care (PoC), Diagnostics.**

I. Introduction

Recently, the use of biosensors has experienced rapid growth for applications like point-of-care (PoC) testing, disease diagnosis, and immunoassays, [1]. The PoC diagnostic provides a convenient way to diagnose diseases everywhere towards personalised healthcare technologies, for home and clinical deployment. These portable devices are used for fast and early detection of diseases and for treatments efficiency optimisation. As an example, among many other applications, biosensors are more widely used in PoC systems for cancer cells early detection, [2]. There are various pioneer technologies in the development of biosensor-based diagnoses, like magnetic, ultrasonic, photonics, and others. A magnetic-based immunoassay is a type of diagnostic tool that uses magnetic beads as labels, involving specific bindings of an antibody and its antigen. In this process, magnetic sensors are used for antibody–antigen binding selection and localisation, [3-5]. Recent advances have allowed the integration and multiplexing of magnetic sensors onto sub-mm CMOS chips toward magnetic-based diagnostics miniaturisation, [6-8].

This paper focuses on magnetic-based biosensors for localisation and detection of paramagnetic particles using giant magnetoresistance (GMR) sensors as an optimal choice for PoC applications due to their high sensitivity and low offset. Table I summarises and compares the main features of recent miniaturised GMR-based biosensing systems, including this work, [9-13]. Fig. 1 conceptually illustrates the basic multi-layered structure of GMR sensors: it consists of two magnetic material layers sandwiching a non-magnetic interlayer. The magnetic layers are designed to have an anti-ferromagnetic coupling (i.e., the magnetisation of these layers is opposite to each other when there is no external magnetic field applied to the material). Extending the preliminary work reported in [14], this paper presents the results from an extensive physical simulation, extends the number of sensors in the array from 3 × 3 to 4 × 4, and provides guidelines for sensors calibration and performance optimisation. The employed 4 × 4 sensors array are off-the-shelf GMR chips. The achieved simulation and experimental results demonstrate the effectiveness of the approach for future miniaturised magnetic-based diagnostics. This approach is

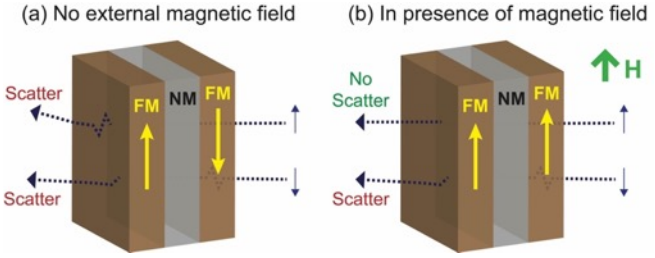

Fig. 1. Working principle of GMR multilayers structures.

This paper is an extended paper from the one presented in the 2017 IEEE Sensors Conference, held at Glasgow, UK on 30/10 – 01/11 2017.
The authors acknowledge support of the Royal Society under grant "MAGLAB" RSG\R1\180269.

Zhaochen Yin was with Microelectronics Lab (meLAB) in the School of Engineering at the University of Glasgow, G12 8QQ, UK. He is now with the Department of Electrical, Computer and Biomedical Engineering, University of Pavia, Italy (e-mail: zhaochen.yin01@universitadipavia.it).

Hadi Heidari is with Microelectronics Lab (meLAB) in the School of Engineering at the University of Glasgow, G12 8QQ, UK. (e-mail: Hadi.Heidari@glasgow.ac.uk).

Edoardo Bonizzoni is with the Department of Electrical, Computer and Biomedical Engineering, University of Pavia, 27100, Italy (e-mail: edoardo.bonizzoni@unipv.it).

TABLE I: COMPARISON OF THE STATE-OF-THE-ART GMR-BASED BIOSENSING SYSTEMS

Type	Detection	Sensor Array	Sensitivity	Application	Reference
GMR Biosensor Array	Magnetorelaxation	8 × 10 GMR sensor array	1 Ω/Oe.	Point-of-Care (PoC) diagnostics platform.	[8]
Integrated GMR biosensor	Biomarkers	N/A	Sensitive detection of AFP from 1 to 10 ng/ml	GMI-based MIA in clinical trials	[9]
Frequency-shift magnetic biosensors	Single-bead sensitivity	8 parallel sensor cells	80 beads	Point-of-Care (PoC) molecular-level diagnosis	[10]
3D field sensor with single bridge of spin-valve GMR films	Biomarkers	N/A	B_X 30V/T B_y 18V/T B_z 8.5V/T	Electronics, electrical, and navigation	[11]
CPP-GMR Spin-Valve Sensors	Magnetic bits	N/A	R/R up to 14% w	Ultra-high-density magnetic recording	[12]
GMR Sensors Array	Ferrofluid	4 × 4 sensor array	2 T^{-1}	Cell detection and localisation	This work

particularly remarkable in comparison with the existing bulky and costly diagnostic systems.

This paper is organised as follows. A brief state-of-art overview of recently reported magnetic-based biosensors including biomagnetic sensing and cell detection is presented in Section II. Section III describes the design and the main features of the selected sensors, of the electronic interface, and the used Halbach cylinder. Section IV provides detailed simulation results of the cell detection achieved with GMR sensors, along with the uniform magnetic field generated by the designed Halbach cylinder. Section V discusses the collected experimental results, while the key outcomes are finally summarised in Section VI.

II. GIANT MAGNETORESISTANCE BIOSENSORS

GMR sensors can be conveniently used for biological and chemical targets detection. However, before detection, magnetic particles immobilisation on the sensor has to be performed. This is commonly achieved by exploiting biomolecular interactions (e.g., antigen-antibody), and thus requires functionalisation via biological or chemical treatments. This Section provides a brief overview of the state-of-the-art for both bio-magnetic sensing and cell detections.

A. Biomagnetic Sensing

A biosensor is a device for analysis that uses an electronic output signal, generated by a biological molecular recognition component, to drive a transducer, [15]. Magnetoresistive biosensors provide a promising method for biomedical detections: they use magnetic particles to localise and sort diagnoses. Such sensors offer a low-cost, fast and robust sensing system with higher sensitivity when compared with enzyme-linked immunosorbent assays and fluorescence-based methods which are nowadays widely used in clinical environments, [16]. Magnetoresistive biosensors are at the state-of-the-art studied in three directions: *(i)* develop the synthesis of magnetic beads that can have the same characteristics of microarrays; *(ii)* employ biosensors in high-resolution, on-chip electrostatic or magnetic field gradient architectures, which can manipulate functionalised single magnetic beads; and *(iii)* employ biocompatible solid-state biosensors for quantifying magnetic beads, [17].

In the last few years, magnetoresistance biosensing platforms such as GMR and tunnelling magnetoresistance (TMR) sensors experienced rapid growth and can be employed in a wide variety of medical applications: point-of-care clinical diagnostics, developments in pharmaceutical drugs, DNA analytics, etc., [18]. However, accurate analysis of biological samples needs further process and trained technicians, increasing both the cost and the time of the measurement. This paper provides a significant improvement in overcoming the above limits proposing a portable and rapid GMR biosensor platform with calibration and localisation algorithm.

B. On-Chip Cell Detection

Due to the universalisation and request of robust and portable biosensors, there is a tremendous demand for lab-on-chip products that do not need expensive specialised equipment or personnel to perform the analysis. This brings in the need for methods to separate, to manipulate, and to move specific particles to specific positions. Microfluidics has been a conventional method for particles manipulation, but there have been studies on using magnetic sensor-manipulator systems as selective and fast analytical devices, [19, 20]. On-chip GMR sensors represent a powerful and low-power sensing system choice featuring high sensitivity and making cell detection easy-to-use and faster. Other healthcare technologies based on on-chip GMR sensors for early detection of diseases have been developed over past years, [21]. Furthermore, due to the fast development of very large-scale integration technologies and multiplex technologies, the fabrication cost of GMR-based sensors significantly reduced. GMR sensors can be conveniently arranged in a large array to determine the location of cells by detecting the difference of the magnetic field density from adjacent sensors, [22, 23].

GMR sensors, by measuring the magnetic field generated by magnetic particles binding to the cells, open potential applications in biological cell sorting and localisation. For example, it has been demonstrated that GMR-based biosensors can detect the influenza A virus, [21], and can quantify the kinetics of antibody–antigen binding, [24].

III. Design and Implementation

The developed prototype includes GMR sensors with readout interface and Halbach cylinders to generate the required uniform magnetic field. The Halbach cylinders have been custom designed, 3D printed, and arranged suitably around the sensors array. Ideally, all the sensors should provide the same output value in the presence of the generated uniform magnetic field. The ferrofluid has been used in a pipette to emulate magnetic nanoparticles. GMR sensors measure the magnetic field via a change in the sensor resistance, thereby enabling cells detection and localisation.

Sensors Selection

This experiment aims to realise the function of cell localisation and sorting. Two types of analogue and digital GMR sensors have been considered. The analogue sensor can read the magnetic flux density to display changes of the magnetic field as an analogue output signal. On the other hand, the digital GMR sensor can detect the magnetic field and show its actual value in a digital format. This experiment needs to read the magnetic field variations and then determine its applicable strength. Therefore, the analogue GMR sensor is the optimal choice to demonstrate the magnetic field variations as an output signal based on the flux density. This project uses off-the-shelf NVE's analogue GMR sensors with 12%-16% resistance change, as a model choice for proof-of-concept, [25].

Hysteresis

The ferromagnetic materials in GMR multilayer are prone to the hysteresis, i.e. a given magnetisation is not reset when the imposed magnetising field is removed.

Hysteresis represents an issue in applications in which the applied magnetic field varies randomly, like in the case here considered for cell detection and localisation. Particularly, in this case of the design, hysteresis causes an offset in the output voltage of the sensors readout circuits. Indeed, with 5-V power supply, a single cube magnet was used to test the hysteresis. The measured saturated value and the hysteresis value have been 0.27 V and 0.01 V, respectively. However, thanks to the large linear range and high sensitivity of the GMR sensors, the 4% hysteresis error at the output voltage is acceptable and provides enough accuracy for localisation.

Uniform Magnetic Field

This experiment, as mentioned, utilises a ferrofluid, magnetised in a uniform magnetic field. There are two methods to generate a uniform magnetic field: using a Helmholtz coil, or using Halbach cylinders. Since the Helmholtz coil is too bulky to be used in a portable device, to minimise the system size, a custom 3D printed Halbach cylinder, consisting of 16 cube magnets, [26], has been employed in our design approach.

The design of the Halbach cylinder has been optimised through extensive finite-element method (FEM) based simulations, which considered different diameters ranging from 3.3 cm to 5 cm. The custom cylinder has been designed in SolidWorks. The 3D printed Halbach cylinder is portable and generates a uniform magnetic field up to 700 mT.

IV. Simulation Results

FEM allows taking into account nonlinear magnetic properties, detailed geometries and distributed currents excitation. Therefore, it offers high accuracy in electromagnetic design in comparison to other methods. In this design, the software COMSOL Multiphysics has been used to run the finite element analysis to fine-tune, verify, and evaluate the performance of the Halbach cylinder and the ferromagnetic beads positioning on top of the GMR sensors.

In the Halbach cylinder simulations, 16 cube magnets were considered and modelled to generate the required uniform magnetic field. For each magnet, the angle difference is considered as 22.5 degrees with 45 degrees rotation. Simulations ensure that the cylinder can adequately generate a uniform and stable magnetic field for operating the GMR sensors at their sensitivity axis. In the simulations, the considered environment is air and all the boundaries are set at a zero-potential point. The magnets embedded in the Halbach cylinder were N42 neodymium magnets that are strong and versatile cube magnets with the size of 10×10×10 mm. **Fig. 2** shows the simulation results collected from COMSOL for Halbach cylinders with different radius. The magnets position on the cylinder was localised correctly based on calculations, and confirmed by COMSOL simulations. It can be noted that it is possible to generate a uniform magnetic field over 95% of the internal diameter of the cylinder. To avoid the interference of non-uniform magnetic field in the edges of the cylinder, a stable 3D printed cage has been used where the Halbach cylinder is placed at the top.

Furthermore, COMSOL has been used to investigate the considered GMR sensor behaviour over a specific position of ferrofluid particles. The simulation results are used to find out an optimised solution for detection of ferromagnetic beads. The simulation results in **Fig. 3** show the operated

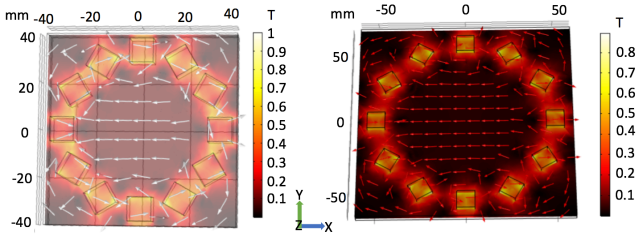

Fig. 2. (left) COMSOL simulation result for the Halbach cylinder (radius 3.3 cm), (right) COMSOL simulation result for the Halbach cylinder (radius 5 cm).

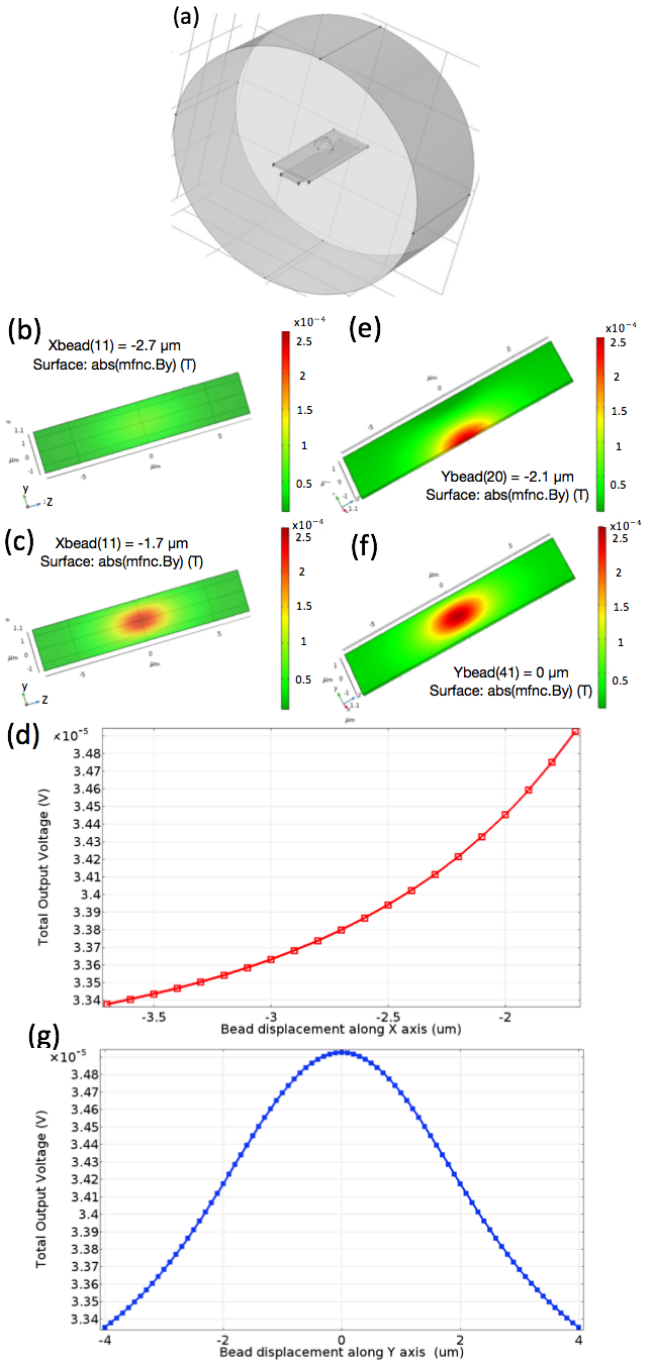

Fig. 3. (a) The model box structure of the magnetic biosensor in COMSOL. (b)-(c) The total output voltage while the ferromagnetic bead moves at X axis and (d) output voltage of the bead along X axis. (e)-(f) The total output voltage while the ferromagnetic bead moves at Y axis and (g) output voltage of the bead along Y axis.

movements of ferromagnetic beads on top of GMR sensors following two trajectories (X and Y axis). The model box built in this simulation is a cylinder instead of a cube to avoid any error due to the different boundary shape. The radius of this cylinder is 20 µm and its height is 15 µm. The work plane of this cylinder is the XY plane. The material of the model box is defined to be air. The GMR sensor is modelled inside the model box with 3-µm width, 15-µm depth, and 0.3-µm height. For real sensor devices, the structure of the GMR element has several layers with different materials, but in simulation, the material was set to be Permalloy which is a nickel (about 80%) and iron (about 20%) magnetic alloy.

The X trajectory moves the magnetic bead from one extreme to a position close to the conducting line. The result shows that when the magnetic bead moves, the stray field produced by the magnetic bead is increased. As a result, the output voltage is increased as well. The Y trajectory moves the magnetic bead from one edge of the conducting line to another edge with the same distance between the bead and the conducting line. During this movement, the simulated output voltage is reported in **Fig. 3(f)** and ranges between 33.4 µV and 34.9 µV. As a result, the measured magnetic flux density on the GMR sensor is affected by the conducting lines. The simulated Y components of the magnetic flux density on the surface of the conducting line and of the GMR are 2.8948 mT and 2.5587 mT in average, respectively.

V. Experimental Results

The fabricated prototype includes two boards; one hosts the array of GMR sensors covered by a protective coating layer and the other is dedicated to the electronic readout circuit interface. **Fig. 4** shows the boards arrangement and a picture of the prototype. The sensory board includes pins for proper connections between the readout circuit and the sensors. The two boards are surrounded by 3D printed Halbach cylinder.

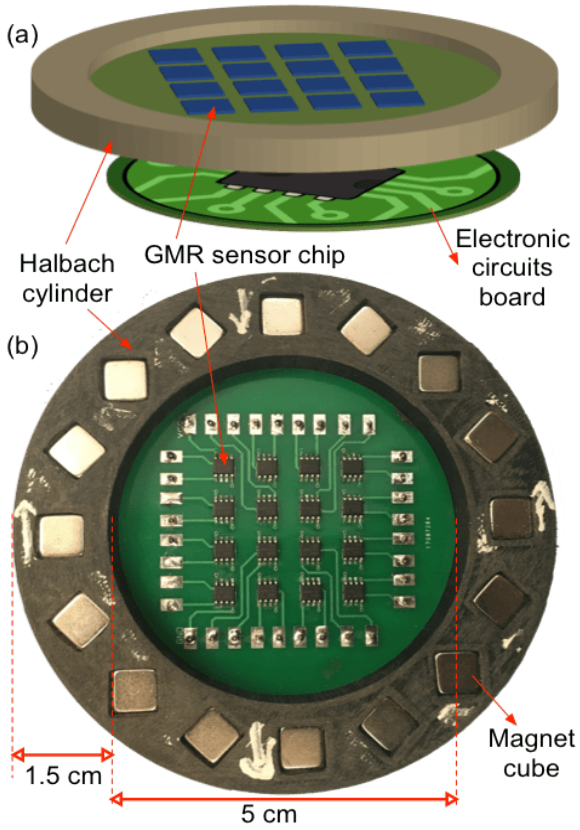

Fig. 4. (a) Final prototype multi-level including the sensory and electronic circuits boards. (b) Top view of the developed 4×4 sensors array surrounded by the 3D printed Halbach cylinder.

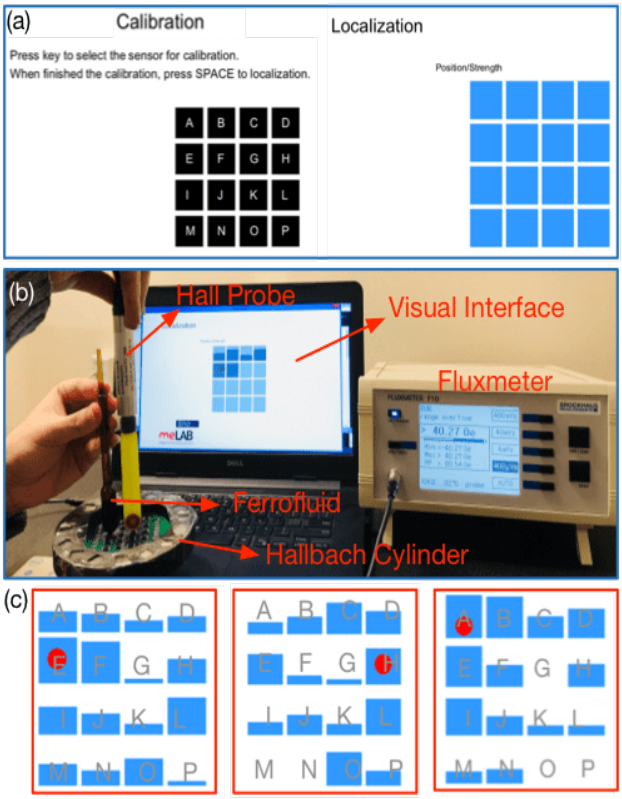

Fig. 5. (a) Visual interface design for calibration and localisation. (b) Test setup and (c) ferrofluid detection and localisation for 4×4 sensors detect system at different positions.

Sensor Calibration and Localisation Algorithm

The sensors, in an array configuration mounted onto the surface of the board, will never be in a perfectly uniform arrangement. Additionally, they will never altogether sense a perfectly uniform field. Calibration is performed to overcome such issues and to avoid mismatch among sensors so that all the sensors will have a similar range to work with.

In this project, the sensors will be calibrated by initially finding the maximum value of the sensor, and then subtracting the baseline value. This will give to each sensor a viable operating range. The localisation algorithm will then be created under the assumption that the operating range will function similarly for all of the calibrated sensors. For example, a magnet is placed in a specific distance from sensor *'1'*, and sensor *'1'* gives an output of 50% its operating range. Now if sensor *'2'* is brought in from a large distance until it also gives an output of 50% its operating range, then the distance between sensor *'1'* and the magnet, and sensor *'2'* and the magnet should be the same.

Various algorithms for localisation in both 2D and 3D space have been developed to minimise errors, optimise location and detection, and provide comprehensive guides on producing tracking mechanisms [27, 28]. For this project, a simpler algorithm was designed in order to ensure a working model was developed on time. The algorithm is implemented with two functions for cell detection and localisation. The 4×4 GMR sensor array configuration is utilised in this project, and then the detection can be realised by comparing the magnetic field changes with the biological data to distinguish the cells. It can also be applied to collect the magnetic field data in specified cells for cell sorting and patterning.

The algorithm used in this project is referred to as weighted average algorithm. It works by using the output of the sensors to "pull" a circle towards its specific coordinates. The stronger the output, the higher weighting will be given to that particular sensor, resulting in a stronger pull. Mathematically, the situation can be modelled as follows:

$$x_{wa} = \sum_{1}^{n} \frac{v_i}{\max v_i - \min v_i} \cdot x_i \quad (1)$$

$$y_{wa} = \sum_{1}^{n} \frac{v_i}{\max v_i - \min v_i} \cdot y_i \quad (2)$$

where x_{wa} and y_{wa} are the weighted positions of the detection point at X axis and Y axis respectively. i refers the number of the sensor and V_i is the output voltage of the i-th sensor. This algorithm is suitable for large sensor array because it will diminish the shift in detection.

The developed software comprises a user interface that helps calibrating the system and easily visualizing the cell localisation. The GMR sensors need to be calibrated before entering the localisation procedure. The calibration interface panel allows the user in choosing the number of sensors (**Fig. 5(a)** and **5(b)**) and allows registering for each sensor its maximum and minimum output voltage value. The maximum value is measured when the ferrofluid is placed on top of the sensor, while the minimum value is recorded in the absence of the ferrofluid. These values will be accounted for during the localisation procedure. The localisation user interface is reported in **Fig. 5(c)**. The matrix represents the 16 sensors (labelled from A to P) and their placement. A bar, associated to each sensor, displays the strength of the GMR sensor while the red point specifies the position of ferrofluid.

The software has been implemented and coded in a microcontroller for data collection. The Processing Development Environment (PDE) was used to sketch the 2D visual interface, [29]. The implemented codes include six segments: display data, pages, serial, calibration, classification and localisation.

Test and Measurement

For comparison with the FEM simulation results in Section IV, various measurements were taken of both the magnets themselves and various locations inside the Halbach cylinders. For the tests of only magnets, the field was measured by touching the Brockhaus Hall probe (Field Coil) to the top of the magnet. The Hall probe was moved around to find the spot of highest magnetic flux density. It is essential to account for the imperfections that are present in all permanent magnets, and so an average value was obtained from after measuring four different magnets to be 0.32 T. In average, the actual field strength values are >90% of the FEM field strength. This indicates a good agreement between the measurements and simulations. The existing difference is

probably because of the magnetic material parameters for N42 neodymium which is used during FEM analysis, found not the same as the parameters of the actual magnet.

Fig. 6 shows the measured stable and accurate outputs collected from the 4×4 sensor array with both magnet and ferrofluid. The system can be fully or partially calibrated. In the full calibration mode, both minimum and maximum values are calibrated, while the partial calibration mode assumes zero as minimum value. By comparing the actual location of the ferrofluid source with the acquired digital output, mean standard deviation (SD) errors of 2.45 (1.61) mm and 5.45 (1.82) mm were observed in full calibration (FC) and partial calibration (PC), respectively. This corresponds to mean error areas of 3.0% and 14.9%, respectively, calculated on the 25×25 mm^2 array surface. In the case of used magnet source, the measured mean errors have been 1.48 (1.14) mm and 1.62 (1.26) mm in FC and PC, respectively. These correspond to mean error areas of 1.1% and 1.3%. Although the error in PC ferrofluid test is high, the rest of detection results shows consistent and precise localisation. This illustrates the importance of proper calibration and also demonstrates the effectiveness of the proposed approach for both a robust ferromagnetic source and a paramagnetic material.

The sensitivity (S) of the sensor can be estimated with the following expression

$$S = \frac{V_{in}}{B} \qquad (3)$$

where V_{in} is to the measured output voltage and B is the detected magnetic field.

Fig. 7(a) and **7(b)** illustrate the measured sensitivity in the presence of a uniform magnetic field. It ranges from 0.2 to 2.3 V/T and from 0.9 to 3 V/T in absence or presence of the ferrofluid, respectively. In this experiment, the sensors have already been calibrated. However, due to the PCB design and fabrication, the sensitivity it might be changed. To make sure that the output for each GMR sensor can be reliable on detection without large shift, the sensitivity test has been performed under the uniform magnetic field with and without ferrofluid. The sensitivity variation for each sensor is not significant (less than 0.2 V/T). This small change will not affect the position shift on detection result significantly. These results also confirm that the measured voltages at the output of the GMR sensors are higher in presence of the ferrofluid, as outlined in **Fig. 7(c)**. Besides, notice that all the measured sensors exhibit the same behaviour. The only exception is sensor number 15 that shows a negative voltage because of voltage fluctuation.

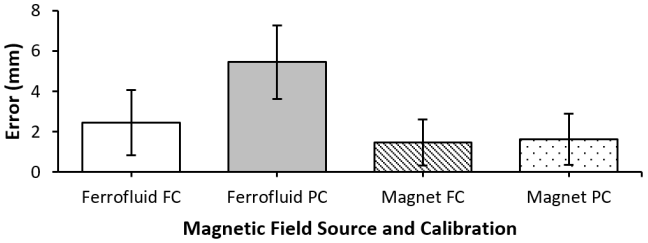

Fig. 6. Comparison of error in localisation from actual position for different magnetic sources and calibrations. Ferrofluid tests show mean (SD) of 2.45 (1.61) mm and 5.45 (1.82) mm for FC and PC. Magnet tests give 1.48 (1.14) mm and 1.62 (1.26) mm.

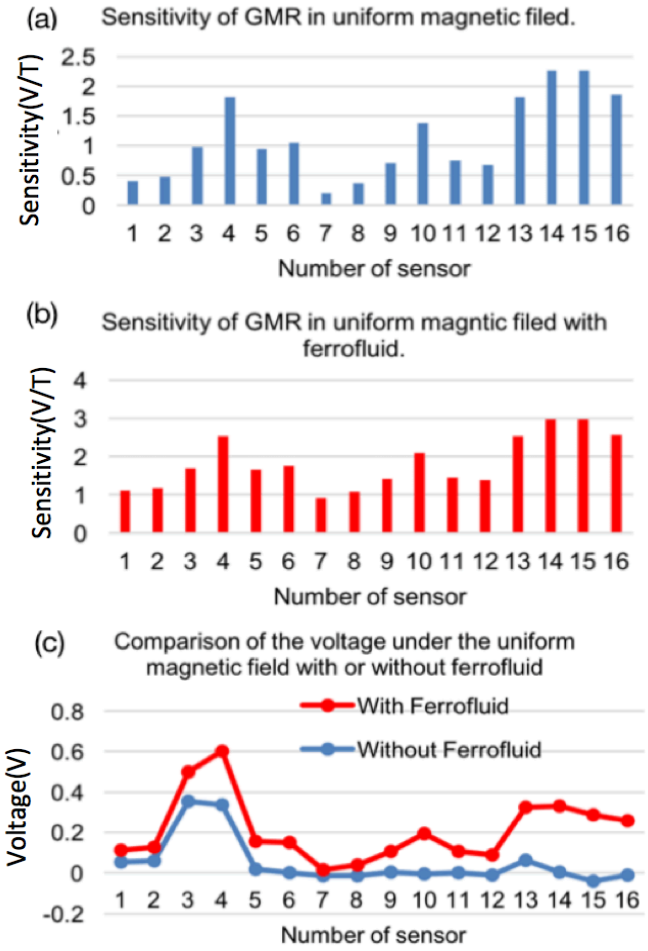

Fig. 7. Measured sensitivity of GMR in uniform magnetic field (a) without and (b) with ferrofluid. (c) Comparison of the voltage measured in presence of uniform magnetic field with or without ferrofluid.

VI. Conclusion and Outlook

This paper presented the design of a prototype developed for on-chip cell detection and localisation based on magnetic sensors. The sensory board includes a 4×4 GMR sensors array. The ferrofluid and a customised 3D printed Halbach cylinder was employed to simulate the magnetic field change in the bead. Sensory chips could detect an average magnetic sensitivity of 2 V/T at room temperature. The implemented algorithm helps in achieving higher sensitivity, positioning speed, and also accurate calibration of the GMR sensors.

As future work, the GMR sensors will be integrated into a single chip using standard CMOS technology, and the results will be compared with the measured data in this paper. The miniaturisation will provide a 3D environment rather than a 2D one in sensor testing for the applications of cell sorting and actual distance determination.

REFERENCES

[1] A. Niemz, T. M. Ferguson, and D. S. Boyle, "Point-of-care nucleic acid testing for infectious diseases," *Trends in biotechnology,* vol. 29, pp. 240-250, 2011.

[2] F. T. Fischbach and M. B. Dunning, *A manual of laboratory and diagnostic tests*: Lippincott Williams & Wilkins, 2009.

[3] V. Nabaei, R. Chandrawati, and H. Heidari, "Magnetic Biosensors: Modelling and Simulation," *Biosensors & Bioelectronics,* 2018.

[4] M. D. Tarn and N. Pamme, "On-Chip Magnetic Particle-Based Immunoassays Using Multilaminar Flow for Clinical Diagnostics," *Microchip Diagnostics: Methods and Protocols,* pp. 69-83, 2017.

[5] D. A. Hall, R. S. Gaster, T. Lin, S. J. Osterfeld, S. Han, B. Murmann*, et al.*, "GMR biosensor arrays: A system perspective," *Biosensors and Bioelectronics,* vol. 25, pp. 2051-2057, 2010.

[6] H. Heidari, E. Bonizzoni, U. Gatti, and F. Maloberti, "A CMOS Current-Mode Magnetic Hall Sensor With Integrated Front-End," *IEEE Trans. Circuits Systems I-Regular Papers,* vol. 62, pp. 1270-1278, 2015.

[7] H. Heidari, E. Bonizzoni, U. Gatti, F. Maloberti, and R. Dahiya, "CMOS vertical Hall magnetic sensors on flexible substrate," *IEEE Sensors Journal,* vol. 16, pp. 8736-8743, 2016.

[8] K.-M. Lei, H. Heidari, P.-I. Mak, M.-K. Law, F. Maloberti, and R. P. Martins, "A Handheld High-Sensitivity Micro-NMR CMOS Platform With B-Field Stabilization for Multi-Type Biological/Chemical Assays," *IEEE J. Solid-State Circuits,* vol. 52, pp. 284-297, 2017.

[9] X. Zhou, C.-C. Huang, and D. A. Hall, "Giant magnetoresistive biosensor array for detecting magnetorelaxation," *IEEE transactions on biomedical circuits and systems,* vol. 11, pp. 755-764, 2017.

[10] T. Wang, Z. Yang, C. Lei, J. Lei, and Y. Zhou, "An integrated giant magnetoimpedance biosensor for detection of biomarker," *Biosensors and Bioelectronics,* vol. 58, pp. 338-344, 2014.

[11] H. Wang, Y. Chen, A. Hassibi, A. Scherer, and A. Hajimiri, "A frequency-shift CMOS magnetic biosensor array with single-bead sensitivity and no external magnet," in *Solid-State Circuits Conference-Digest of Technical Papers, 2009. ISSCC 2009. IEEE International*, 2009, pp. 438-439,439 a.

[12] V. Luong, J. Jeng, B. Lai, J. Hsu, C. Chang, and C. Lu, "Design of three-dimensional magnetic field sensor with single bridge of spin-valve giant magnetoresistance films," in *Magnetics Conference (INTERMAG), 2015 IEEE*, 2015, pp. 1-1.

[13] T. Nakatani, S. Li, Y. Sakuraba, T. Furubayashi, and K. Hono, "Advanced CPP-GMR Spin-Valve Sensors for Narrow Reader Applications," *IEEE Transactions on Magnetics,* vol. 54, pp. 1-11, 2018.

[14] S. Samyak and H. Heidari, "On-chip Magnetoresistive Sensors for Detection and Localization of Paramagnetic Particles," in *Proc. of IEEE SENSORS Conference*, Glasgow, UK, 2017.

[15] P. R. Coulet, "What is a biosensor," *Chapter 1; Biosensor principles and applications,* pp. 1-6, 1991.

[16] L. Marri, A. M. Jansson, C. E. Christensen, and O. Hindsgaul, "An enzyme-linked immunosorbent assay for the detection of diacetyl (2, 3-butanedione)," *Analytical Biochemistry,* 2017.

[17] N. M. M. Pires, T. Dong, U. Hanke, and N. Hoivik, "Recent developments in optical detection technologies in lab-on-a-chip devices for biosensing applications," *Sensors,* vol. 14, pp. 15458-15479, 2014.

[18] L. Moro, M. Turemis, B. Marini, R. Ippodrino, and M. T. Giardi, "Better together: Strategies based on magnetic particles and quantum dots for improved biosensing," *Biotechnology advances,* vol. 35, pp. 51-63, 2017.

[19] C. Albon, A. Weddemann, A. Auge, K. Rott, and A. Hütten, "Tunneling magnetoresistance sensors for high resolutive particle detection," *Applied Physics Letters,* vol. 95, p. 023101, 2009.

[20] J. Schotter, P. B. Kamp, A. Becker, A. Puhler, G. Reiss, and H. Bruckl, "Comparison of a prototype magnetoresistive biosensor to standard fluorescent DNA detection," *Biosensors & Bioelectronics,* vol. 19, pp. 1149-1156, May 15 2004.

[21] V. D. Krishna, K. Wu, A. M. Perez, and J.-P. Wang, "Giant magnetoresistance-based biosensor for detection of Influenza A Virus," *Frontiers in microbiology,* vol. 7, p. 400, 2016.

[22] S. M. Thompson, "The discovery, development and future of GMR: The Nobel Prize 2007," *Journal of Physics D: Applied Physics,* vol. 41, p. 093001, 2008.

[23] C.-C. Huang, X. Zhou, and D. A. Hall, "Giant Magnetoresistive Biosensors for Time-Domain Magnetorelaxometry: A Theoretical Investigation and Progress Toward an Immunoassay," *Scientific Reports,* vol. 7, p. 45493, 04/04/online 2017.

[24] R. S. Gaster, L. Xu, S.-J. Han, R. J. Wilson, D. A. Hall, S. J. Osterfeld*, et al.*, "Quantification of protein interactions and solution transport using high-density GMR sensor arrays," *Nature Nanotechnology,* vol. 6, p. 314, 04/10/online 2011.

[25] N. Corporation, *GMR Sensors Data Book*: Eden Prairie, 2003. Available: https://www.nve.com/ [Accessed 25/02/2018].

[26] Z. Zhu and D. Howe, "Halbach permanent magnet machines and applications: a review," *IEEE Proceedings-Electric Power Applications,* vol. 148, pp. 299-308, 2001.

[27] O. Talcoth and T. Rylander, "Optimization of sensor positions in magnetic tracking," Chalmers University of Technology.

[28] A. Farajidavar, J. M. Block, and M. Ghovanloo, "A comprehensive method for magnetic sensor calibration: a precise system for 3-D tracking of the tongue movements," presented at the Conf Proc IEEE Eng Med Biol Soc, 2012.

[29] B. Fry and R. Casey, *Processing*, Available: https://processing.org/ [Accessed 01/03/2018].